



## Building Extraction from WorldView-2 Images Using Invariant Color Models

Faten Mostafa<sup>1</sup>, Yasser Mostafa<sup>1</sup>, Mahmoud Nokrashy O.Ali<sup>2</sup>, Mohamed Yousef<sup>3</sup>

<sup>1</sup>Civil Eng. Dept. Faculty of Engineering, Sohag University, Sohag, Egypt

<sup>2</sup>Civil Eng. Dept. Faculty of Engineering, Al-Azhar University, Cairo, Egypt

<sup>3</sup> Mining and Metallurgical Eng. Dept. Faculty of Engineering, Assiut University, Assiut, Egypt

### الملخص العربي:

تعتبر عملية استخراج المباني من صور الأقمار الصناعية هامة جدا لتحديث الخرائط وقواعد بيانات نظم المعلومات الجغرافية. ولكن نظرا للطبيعة غير المتجانسة للمباني في المناطق الحضرية وخاصة في البلدان النامية فإن استخراج المباني يعد مهمة صعبة للغاية. تقدم هذه الدراسة مؤشر (معادلة) جديد لتحسين استخراج المباني من صور القمر الصناعي WorldView-2 المكونة من ثمان نطاقات طيفية عن طريق استخدام **Invariant color models**. ثم تم إجراء عملية **Spatial contrast stretch** على الرسم البياني التحليلي لصورة المؤشر الناتجة. تجرى بعد ذلك عملية **Thresholding** لفصل الأبنية عن باقي المعالم الموجودة في الصورة. تم تطبيق المؤشر المقترح على خمس مناطق للدراسة ومقارنته بمؤشرين معتمدين لاستخراج المباني. وقد أظهرت النتائج أن المؤشر المقترح حقق أفضل النتائج (**F-score** بمتوسط 91.26%) وأنه لديه القدرة الذاتية على فصل المباني عن المعالم التي تتقارب مع المباني في الدرجات اللونية.

### Abstract:

Building extraction from satellite images is very important for update maps and GIS databases. However, due to the highly heterogeneous nature of the building in urban areas, especially in developing countries, the extraction becomes a difficult task. In this study, a new image index is developed to improve buildings extraction from worldview eight bands image by employing invariant color models. A special contrast stretch is applied on the resulted image index histogram. Then, the thresholding process is carried out to separate the image into building and non- building area. The proposed index has been applied on five study areas and compared with two standard indices methods for building extraction. The results demonstrated that the proposed index achieves the best results (average F-score of 91.26%) and has the ability to reduce misclassification of buildings with spectral similar areas.

**Keywords:** Building extraction, index, 8-bands, color model, VHR satellite image.

### 1. Introduction

The production and updating of building maps have important security, technical, economic and planning effects to distribute development efforts. The main problems of building detection are their diversity in shape, size, distribution and density. Also, different materials found on the building's rooftops which can be confused with surrounding objects have similar spectral response. Remote sensing satellite images are promising tools for

feature extraction. The new generation of the remote sensing satellites has been developed to capture the images with high spatial and spectral resolution. The finer resolution data helps in improving detection of land cover classes.

Some scientific studies have been concentrated on developing spectral indices for building enhancement from satellite images. Sirmacek, and Unsalan, (2008) employed the red and green bands of the color aerial image to produce building detection index. However the main issue is its ability to extract red building's rooftop only. Another building index proposed by Ettarid, and Rouchdi (2008) was developed by employing Value band in Hue-Saturation-Value (HSV) color model with Red band in multispectral image. For high resolution 8-band images some indices have been generated utilizing the capability of the new band. Zhou et al, (2012) created Normalized Difference Brick Roof Index (NDBRI) using Yellow and Green bands of multispectral worldview-2 image. NDBRI gives good results, but however the main limitation that it is developed just for brick rooftop.

Wolf (2012) proposed a normalized difference ratio based on the red edge and coastal blue bands termed WorldView Building Index (WV-BI) for detecting buildings. WV-BI is depending on difference in contrast between manmade areas and the background. Sameen and Pradhan (2016) developed an index named Building Spectral Index (BSI) by selecting the most two significant band for building extraction. By using multi-objective particle swarm optimization, they found that the Yellow and NearInfrared1 bands as the most appropriate bands among the eight ones for built-up area extraction. Both indices have more advantage than the other mentioned ones because they utilize the benefits of spectral properties of the 8-bands image and can be used for different buildings types. The aim of the present study is to develop a new building detection index to improve building extraction from VHR 8-band images.

The rest outlines of this work are organized as follows. In section 2, the methodology to deduce the proposed index is described. Section 3 includes the application of the index on five different study areas. Two powerful indices are employed to the same five study areas for validation purpose as given in section 4. An accuracy assessment process is then applied on section 5. The results and discussion are reported in section 6. Finally, the conclusion and recommendation are found in section 7.

## **2. Methodology**

Buildings are the brightest areas in remote sensing images which make spectral analysis methods useful to differentiate building from other features. As using available multispectral bands directly gives inaccurate detection of building pixels, it will be more convenient to use invariant color models in the building detection process. Moreover, accuracy will go up when the invariant color model defined by certain bands that are selected according to its validation for building area enhancement. The proposed method consists of two stages; the first stage is the generation of a new image index to differentiate between building and non-building pixels. In the next stage, the resulting histogram of the index image is stretched and thresholded to accurately identify the building pixels from the index image.

### **2.1. Building detection index**

Recent studies for spectral reflectance of the main ground features along the eight bands; Coastal-Blue (CB), Blue (B), Green (G), Yellow (Y), Red (R), Red Edge (RE), Near-Infrared1 (NIR1) and Near-Infrared2 (NIR2); have shown that G, Y and RE bands are useful for manmade areas enhancement. Where, Zhou et al. (2012) demonstrated that G

and Y band are effective for building extraction process. Also, Adeline et al. (2013) illustrated that the building has the highest reflectance values in band G, Y and RE with a significant difference from the non-building features. Ahmed 2012 has added, that difference increase in the Y band, where building brightness increase and the brightness values of the other features decrease. Also, DigitalGlobe, 2009 has been declared that there are large spectral disparities in bands G, Y, R and RE.

Intensity-Hue-Saturation (IHS) color space has special properties which make it suitable for a specific application. The main contribution of radiation sent from building to remote sensor is the reflected light, not scattered light. The intensity of reflected light is much stronger than scattered light, which make the building area illumination is sufficient in the brightness component (I) (Guangyao et al., 2013). Consequently, building areas will have the higher value in the intensity channel than the non-building areas. So, I component will be used to highlight building and it will be defined by G, Y and RE bands instead of R, G and B bands. The G, Y and RE bands are converted to I band as follows (ERDAS field guide, 2013):

$$I_{G,Y,RE} = (\text{Max}_{G,Y,RE} + \text{Min}_{G,Y,RE}) / 2 \dots\dots\dots (1)$$

where:  $\text{Max}_{G,Y,RE}$  is the highest reflectance value in the G, Y, and RE bands.

$\text{Min}_{G,Y,RE}$  is the lowest reflectance value in the G, Y, and RE bands.

The normalized histogram of  $I_{G,Y,RE}$  component (Figure 1.a) shows that the digital number (DN) values of light areas are relatively concentrated, but with no significant difference from the darker areas. So, extraction of building is not easy to acquire depending only on thresholding of  $I_{G,Y,RE}$  component histogram because of increasing complexity of surface features in high resolution images. Therefore, the brightness component  $I_{G,Y,RE}$  is gathered only as one of the components to highlight buildings.

Furthermore, the original image will be transformed to Principal Components (PCs) method. The eight bands (CB, B, G, Y, R, RE, NIR1, NIR2) are employed to define the PCs. The first principle component (PC1) includes the largest percentage of information of the total scene incarnated the major differences between various objects in the image data making the image classification process more efficient (Mostafa and Abd-elhafez, 2017). Therefore, PC1 will be employed to increase separation of building class.

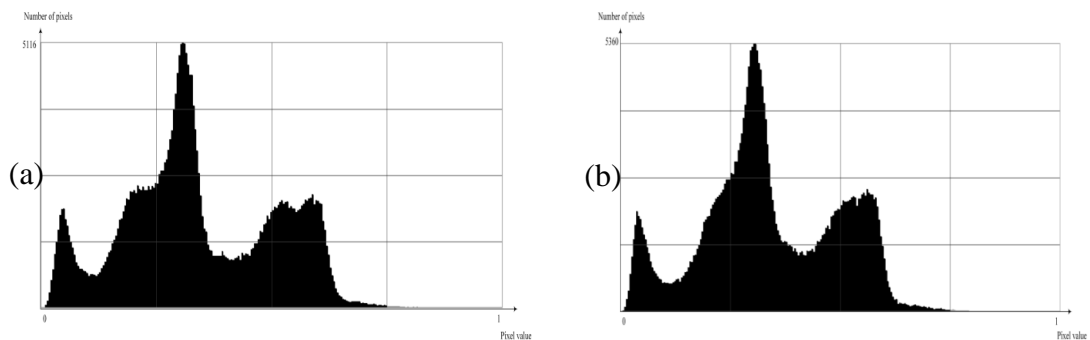


Figure 1: (a) Histogram of normalized  $I_{G,Y,RE}$  band  
 (b) Histogram of normalized PC1 band.

$I_{G,Y,RE}$  and  $PCI$  bands are chosen to enhance the contrast between building and other spectral similar objects. If the digital numbers (DNs) of  $PCI$  band are squared the differences between building DN and the remained features DN are increased. Accordingly, multiplying the squared value of  $PCI$  band by  $I$  band will be effective to deliver large DN values for building pixels and the difference from DN values of the remained features are increased as required. Subtracting the term ( $I_{G,Y,RE}$  Band  $\times$  squared  $PCIBand$ ) from the unity (1) cause the reverse of the image and improve visibility. For each image pixel, the Transformed Building Index (TBI) is calculated by the following formula:

$$TBI = 1 - (I_{G,Y,RE} \text{ Band} \times \text{squared } PCIBand) \dots\dots\dots (2)$$

where:  $I_{G,Y,RE}$  is normalized intensity component of the IHS color space results from G, Y and RE bands.  $PCI$  is normalized value of first principal component band.

## 2.2. Improvement building pixels separation

Certain features can be analyzed in greater radiometric details by assigning the display range exclusively to a particular range of image values. Although the output range of light features from the index image become more concentrated than the output range of dark features, the output range of dark features still devoted entirely to a *small* range of image values as shown in figure 2.a . On the stretch displayed, minute tonal variations in the dark area range would be greatly exaggerated. In this work, a special Contrast Stretch (SCS) is applied on the dark area which depends directly on its minimum (MIN) and maximum (MAX) values. That MIN and MAX can be determined objectively by visual inspection (Yamazaki et al., 2009). On the other hand, the brighter and darker land features, would be “washed up” by being displayed at a single bright level (equal to MAX and MIN, respectively). The histogram of SCS is calculated according to the following equation (Lillesand and Kiefer, 2000):

$$DN' = \left( \frac{DN - MIN}{MAX - MIN} \right) \times 255 \dots\dots\dots (3)$$

where  $DN'$  is the digital number assigned to pixel in output image,  $DN$  is the original digital number of pixel in input image,  $MIN$  is the minimum value of the area of interest in the input image, and  $MAX$  is the maximum value of the area of interest in the input image.

The resulted stretched histogram is used to separate buildings from remaining features close to them in spectral brightness using neighborhood valley-emphasis threshold method proposed by Fan and Lei, (2012). The lowest point after the first peak on the index image histogram is the threshold value to separate building from non-building pixels (see figure 2.b).

## 3. Building extraction with TBI

At the present study, WorldView-2 (WV-2) pan-sharpened image with eight spectral bands and 0.5m resolution was used. The proposed TBI index was tested and evaluated on five study areas selected from the image. The study areas are selected to cover different urban regions contain buildings varying in density, shape, size and colors.

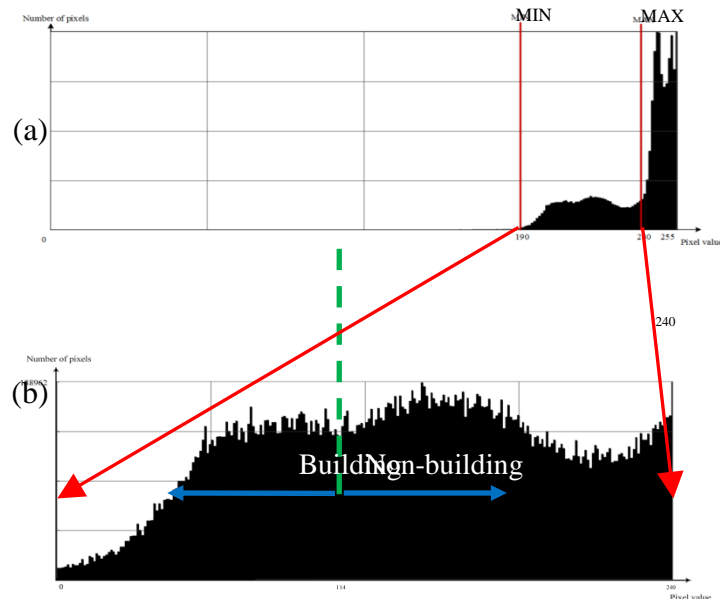


Figure 2: (a) Histogram of TBI image, MIN=190 and MAX=240.  
 (b) Histogram of SCS-TBI image.

Study area A contains low dense urban area with large size buildings (Figure 3) while study area B includes large size buildings with high density (Figure 4). Study area C consists of small buildings with symmetrical shapes and distribution (Figure 5) counter to study area D which contains buildings in different shape, size and distribution (Figure 6). The E area is a high dense residential blocks without separating building units (Figure 7). Most study areas exhibit significantly different colors of the roof with spectral reflectance close to roads and bare soil. TBI index have been programmed and implemented on study areas using ERDAS IMAGINE 2015 model maker. The results are shown in figures 3, 4, 5, 6 and 7 corresponding to the five areas mentioned above, respectively.

#### 4. Standard building detection indices

To validate the proposed TBI index and check its efficiency, the obtained results are compared with two standard indices WorldView Building Index (Wolf, 2012) and Built-up spectral index (Sameen and Pradhan, 2016). The two indices have been developed using the eight band of WV-2 and available in ERDAS IMAGINE 2015. Both are described as follows:

##### 4.1. WorldView Building Index (WV-BI)

Wolf (2012) exploited reflectance response of ground materials along the eight bands of WV-2 to determine the most effective method for processing the information to detect man-made features. He found that the difference between the RE and CB bands will provide an effective means of segregating bright man-made features. Therefore, that is used to discriminate between the building and other features according to the following formula:

$$WV - BI = \frac{(Coastal\ band - Red\ Edge\ band)}{(Coastal\ band + Red\ Edge\ band)} \dots\dots\dots (4)$$

##### 4.2. Building Spectral Index (BSI)

Sameen and Pradhan (2016) introduced a simple two-band ratio index (BSI). BSI was

developed by applying Particle Swarm Optimization (PSO) technique on WV-2 images to select the adequate bands from the eight bands of WV-2 images for built-up detection index. PSO is a computational method which optimizes the index through iterative trials to improve its quality. Their results showed that Y and NIR1 bands are the most appropriate bands among the eight bands for built-up area extraction. Then, the final index was formulated by development a normalized band ratio as follows:

$$BSI = \frac{(Yellow\ band - 2 \times NIR1\ band)}{(Yellow\ band + 2 \times NIR1\ band)} \dots\dots\dots (5)$$

### 5. Accuracy assessment

The results look promising when compared with the reference images in which true buildings are delineated manually through three statistical metrics named recall (R), precision (P) and F-score (F). Many researchers use these definitions to evaluate the efficiency of their system such as Femiani et al. (2015), Gregoris and Stavros (2016), Ngo et al. (2017), Gao et al. (2018). The recall (R) metric indicates the percentage of building pixels correctly detected where the denominator stands for the number of true building pixels. The precision (P) metric gives the percentage of the true detected pixels against the whole detected pixel automatically (ground truth along with the false alarm). F-score (F) is the combination of precision and recall into a single score that gives each one of both metrics an equal importance (weight). These metrics are formulated as follow:

$$R = \{TP / (TP + FN)\} \times 100 \dots\dots\dots (7)$$

$$P = \{TP / (TP + FP)\} \times 100 \dots\dots\dots (6)$$

$$F = (2 \times R \times P) / (R + P) \dots\dots\dots (8)$$

where: TP (true positive) is the number of buildings pixels correctly identified. FN (false negative) is the number of buildings pixels identified as non-building. FP (false positive) is the number of non-building pixels identified as building.

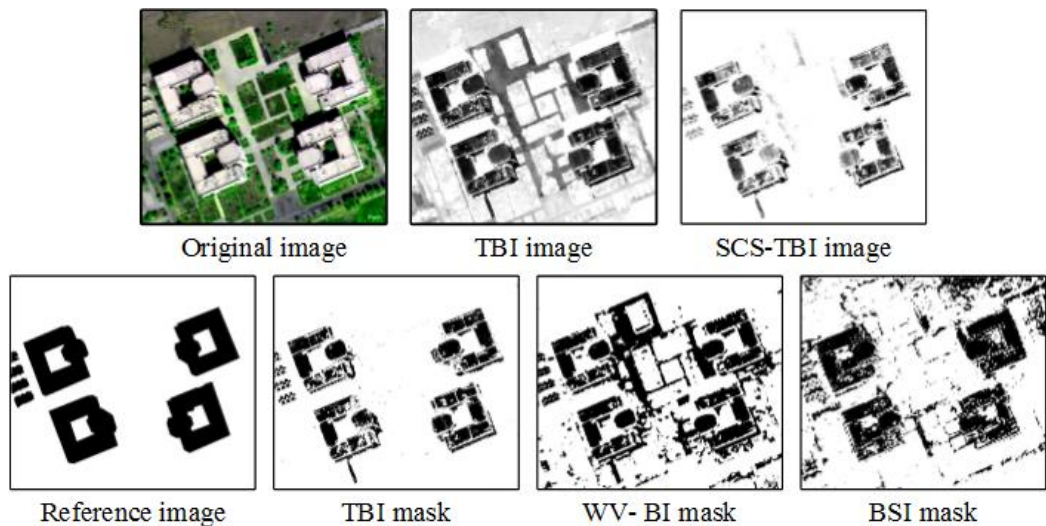


Figure 3: The results of applying the proposed TBI, WV-BI and BSI indices on the study area A



Original image

TBI image

SCS-TBI image



Reference image

TBI mask

WV-BI mask

BSI mask

Figure 4: The results of applying the proposed TBI, WV-BI and BSI indices on the study area B.



Original image

TBI image

SCS-TBI image



Reference image

TBI mask

WV-BI mask

BSI mask

Figure 5: The results of applying the proposed TBI, WV-BI and BSI indices on the study area C.

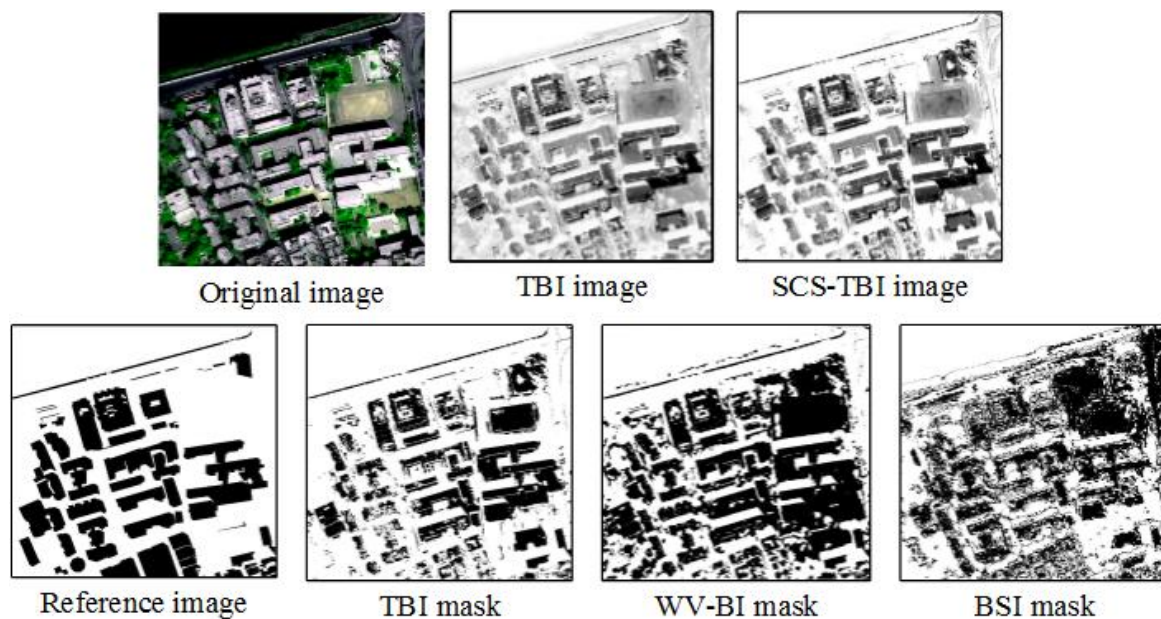


Figure 6: The results of applying the proposed TBI, WV-BI and BSI indices on the study area D.

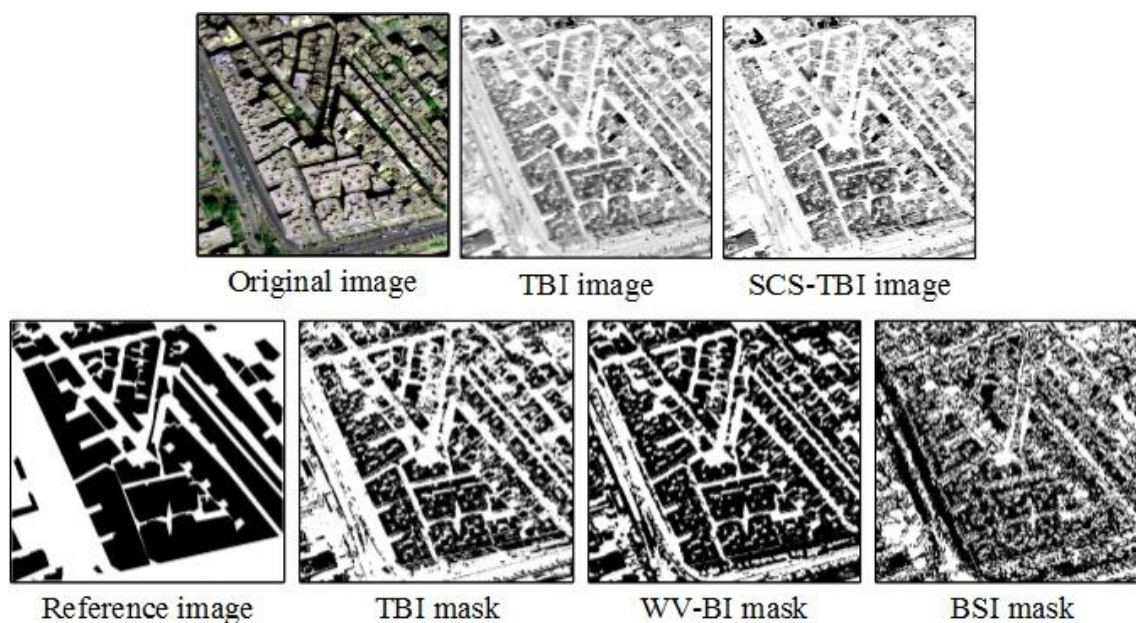


Figure 7: The results of applying the proposed TBI, WV-BI and BSI indices on the study area E.

By comparing the three indices (WV-BI, BSI and The proposed TBI) according to reference ground truth, the accuracy assessment results are scheduled in table (1).

Table 1: Accuracy assessment of WV-BI, BSI and the proposed TBI on the five study areas.

Study area (size, pixels)	WV-BI			BSI			The proposed TBI		
	<i>P</i> (%)	<i>R</i> (%)	<i>F</i> (%)	<i>P</i> (%)	<i>R</i> (%)	<i>F</i> (%)	<i>P</i> (%)	<i>R</i> (%)	<i>F</i> (%)
A (579×490)	81.06	86.51	83.70	85.13	87.11	86.11	95.88	84.21	89.67
B (587×470)	84.37	96.03	89.82	81.26	89.25	85.07	95.43	95.16	95.30
C (437×392)	79.82	93.65	86.18	77.97	84.81	81.24	93.41	92.75	93.08
D (573×546)	82.03	85.63	83.79	84.34	78.68	81.41	91.47	83.93	87.54
E (554×532)	87.16	91.01	89.04	75.11	83.54	79.10	92.01	89.43	90.70
Average	82.89	90.57	86.51	81.16	84.68	82.59	93.64	89.10	<b>91.26</b>

## 6. Results and discussion

From visual inspection, it become clear that TBI mask images are more accurate and sharpness than both WV-BI and BSI mask images. TBI and WV-BI showed better results than SBI along all study areas. From table 1 it can be seen that TBI and WV-BI have the high percentage in the average R (89.10% and 90.57% respectively). It can be said that TBI perform much better than WV-BI in separating building from background (see figures 4 through 8). Although the average R of WV-BI is more than the average R of TBI by 1.5%, TBI far superior to WV-BI in the average of P (93.64% against 82.89%, respectively) .Scanning R and P for TBI and WV-BI in table 1 along all study areas further confirms this result. This means that the proposed TBI can detect building with high accuracy and have self-efficiency to discriminate between building and similar spectral background.

The WV-BI delivered the highest R values for most study areas (86.51%, 96.03%, 93.65%, 85.63% and 91.01%). It performs well in low and high density area with large and small building size. The values of the P metric delivered by WV-BI are smaller than that delivered by TBI for all study areas (81.06%, 84.37%, 79.82%, 82.03% and 87.16%) due to the similarity between buildings and background in spectral properties. WV-BI, therefore, is not able to distinguish between building and areas close to it in brightness.

In regard to BSI, it can be seen that it have average R of 84.68% (ranging from 78.68% to 89.25% corresponding to individual areas). Also, Its P average value is 81.16% for a range from 75.11% into 85.13% (for areas individually). That index delivers lower accuracy than the proposed TBI and illustrates distorted building and non-building areas. Also, for BSI, the similar spectral background is greatly confused with buildings.

On the other hand, the proposed TBI gives high R results with all study areas (ranging from 83.93% to 95.16%). Also, it gives significant progress in P results (ranging 91.47% to 95.88%) regarding the study areas. This means that, the index is able to detect buildings with high accuracy and exclude the confusion with background.

## 7. Conclusion and Recommendation

Based on the results which are represented through figure 2 as well as through figures 3 through 7 and included in table 1, it can be concluded that:

- In general, the proposed index TBI is able to distinguish building pixels from similar spectral background areas.
- Also, that proposed index achieved the highest accuracy with an average F-score of 91.26% compared with 86.16% for WV-BI and 82.59% for BSI.
- Where according to the proposed index, the buildings are classified in the form of individual pixels based on spectral information only, it is recommended to follow that index by mathematical morphology tools to improve rooftop extraction and geometrical shape of buildings.

## 8. References

- Adeline, K. R. M., Chen, M. Briottet, X. Pang, S. K. and Paparoditis, N., 2013. "Shadow Detection in Very High Spatial Resolution Aerial Images: A Comparative Study." *ISPRS Journal of Photogrammetry and Remote Sensing* 80: 21–38. Doi:10.1016/j.isprs.2013.02.003.
- Ahmed, S. 2012. "Second Generation Multi-Resolution Techniques for Edge Detection and Feature Extraction from 8-bands High Resolution Satellite Imagery." PhD Department of Geomatics Engineering, University of Calgary, Alberta. Doi:10.1094/PDIS-11-11-0999-PDN.
- DigitalGlobe., 2009. "The Benefits of the 8 Bands of WorldView-2." Longmont, CO: DigitalGlobe. White Paper.
- ERDAS. 2013. Erdas Field Guide. 5th ed. Atlanta, Georgia: Erdas Inc.
- Ettarid, M., and Rouchdi, M., 2008. "Automatic Extraction of Building from High Resolution Satellite Images." *The International Archives of the Photogrammetry, Remote Sensing and Spatial Information Sciences*, XXXVII (B8).
- Fan, J., L., and Lei, B., 2012. "A Modified Valley-emphasis Method for Automatic Thresholding." *Pattern Recognition Letter*, 33 (6): 703–708.
- Femiani, J., Li, A., Razdan, A., and P. Wonka. 2015. "Shadow-based Rooftop Segmentation in Visible Band Images." *IEEE Journal of Selected Topics in Applied Earth Observation and Remote Sensing*, 8 (5): 2063–2077.
- Gao, X., Wang, M., Yang, Y., and L. Gongquan. 2018. "Building Extraction from RGB VHR Images Using Shifted Shadow Algorithm.", *IEEE Access Open Access Journal*, 6:22034- 22045. Doi: 10.1109/ACCESS.2018.2819705.
- Gregoris, L., and S. Stavros. 2016. "Building Extraction in Satellite Images Using Active Contours and Colour Features.", *International Journal of Remote Sensing* 37(5): 1127-1153. Doi:org/10.1080/01431161.2016.1148283.
- Guangyao, D., G. Huili, Z. Wenji, T. Xinming, and C. Beibei. 2013. "An Index-Based Shadow Extraction Approach on High-Resolution Images." *International Symposium on Satellite Mapping Technology and Application*. Vol. 7, Nanjing Jiangsu. 19–26, Russia, April.

- Lillesand, T., and Kiefer, R., 2000. "Remote Sensing and Image Interpretation", Fourth edition. John Wiley and Sons, Inc. New York. USA.
- Mostafa, Y., and A. Abedehafez., 2017. "Accurate Shadow Detection from High-Resolution Satellite Images." *IEEE Geoscience and Remote Sensing Letters* 14 (4): 494–498. Doi:10.1109/LGRS.2017.2650996.
- Ngo, T.T., Mazet, V., Collet, C., and P. Fraipont. 2017. "Shape-based Building Detection in Visible Band Images using Shadow Information." *IEEE Journal of Selected Topics Applied Earth Observation and Remote Sensing* (99):1-13 10 :920–932. Doi: 10.1109/JSTARS.2016.2598856.
- Sameen, M.I. and B. Pradhan, 2016. "A novel built-up spectral index developed by using multi objective particle-swarm-optimization technique." in *IOP Conference Series: Earth and Environmental Science.. 2016. IOP Publishing.*
- Sirmacek, B., and Unsalan, C., 2008. "Building Detection from Aerial Images Using Invariant Color Features and Shadow Information." *Conference Paper*. November 2008. Doi: 10.1109/ISCIS.2008.4717854. Source: IEEE Xplore.
- Wolf, A.F., 2012. "Using WorldView-2 Vis-NIR Multispectral Imagery to Support Land Mapping and Feature Extraction Using Normalized Difference Index Ratios. " in *Algorithms and Technologies for Multispectral, Hyper-spectral, and Ultra-spectral Imagery XVIII*. International Society for Optics and Photonics.
- Yamazaki, F., W. Liu, and M. Takasaki., 2009. "Characteristics of Shadow and Removal of its Effects for Remote Sensing Imagery." 2009 *IEEE International Geoscience and Remote Sensing Symposium*.
- Zhou, X., Jancso, T., Chen, C., and Verone, M., W., 2012. "Urban Land Cover Mapping Based on Object Oriented Classification Using WorldView 2 Satellite Remote Sensing Images." *International Scientific Conference on Sustainable development & Ecological Footprint* March 2012, Sopron, Hungary.